

pubs.acs.org/ac Article

Solid-Phase Microextraction Enables Isolation of BRAF V600E Circulating Tumor DNA from Human Plasma for Detection with a Molecular Beacon Loop-Mediated Isothermal Amplification Assay

Marcelino Varona, Derek R. Eitzmann, Darshna Pagariya, Robbyn K. Anand, and Jared L. Anderson*



Cite This: Anal. Chem. 2020, 92, 3346-3353



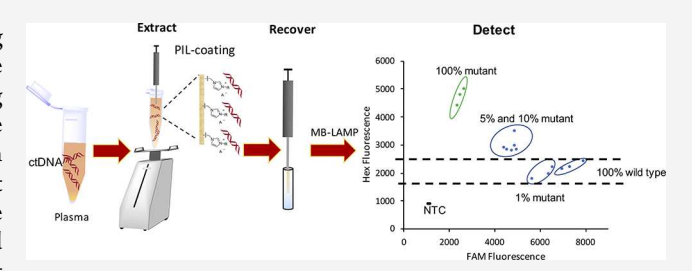
ACCESS

III Metrics & More



s) Supporting Information

ABSTRACT: Circulating tumor DNA (ctDNA) is a promising biomarker that can provide a wealth of information regarding the genetic makeup of cancer as well as provide a guide for monitoring treatment. Methods for rapid and accurate profiling of ctDNA are highly desirable in order to obtain the necessary information from this biomarker. However, isolation of ctDNA and its subsequent analysis remains a challenge due to the dependence on expensive and specialized equipment. In order to enable widespread implementation of ctDNA analysis, there is a need for low-cost



and highly accurate methods that can be performed by nonexpert users. In this study, an assay is developed that exploits the high specificity of molecular beacon (MB) probes with the speed and simplicity of loop-mediated isothermal amplification (LAMP) for the detection of the BRAF V600E single-nucleotide polymorphism (SNP). Furthermore, solid-phase microextraction (SPME) is applied for the successful isolation of clinically relevant concentrations (73.26 fM) of ctDNA from human plasma. In addition, the individual effects of plasma salts and protein on the extraction of ctDNA with SPME are explored. The performed work expands the use of MB-LAMP for SNP detection as well as demonstrates SPME as a sample preparation tool for nucleic acid analysis in plasma.

E arly and accurate detection of cancer is paramount for prompt administration of treatment and positive patient outcomes.¹ Tissue biopsy is the most commonly used technique for the diagnosis of cancer. During a biopsy, tissue suspected of being cancerous is obtained from the patient and subsequently analyzed using microscopy. However, biopsies are time-consuming, invasive, and often difficult to obtain. Moreover, obtaining a sufficient amount of tissue for histological analysis as well as genotyping can present a significant challenge. As a result, minimally invasive methods that can provide rapid results are highly desirable for reliable diagnosis and treatment of cancer.

Circulating tumor DNA (ctDNA) represents a promising biomarker for the diagnosis of cancer and monitoring of treatment efficacy. ^{2,3} The genomic profile of ctDNA provides dynamic insight into the tumor's genetic makeup. Since ctDNA can be found in blood and plasma, it can be obtained from patients with more frequency while being significantly less invasive than traditional tissue biopsies. This has led to the popularization of personalized medicine, an approach which seeks to tailor medical treatment in an individual rather than a "one size fits all" basis, as a strategy for the development of more effective therapies.⁴

Vemurafenib is a representative example of an anticancer drug that was developed to combat metastatic melanomas that specifically possess the BRAF V600E mutation.⁵ The mutation is caused by the substitution of a thymine (T) base with

adenine (A) within the gene encoding for BRAF — a serine/threonine protein kinase that promotes cell mobility and proliferation. The resulting mutation causes the amino acid to change from valine (V) to glutamate (E), promoting an increase in activity of the protein. Up to 90% of BRAF mutant melanomas contain this specific mutation.^{6,7} Not only is this mutation relevant for melanomas, it has also been observed in various other cancers including lung adenocarcinomas.⁸ Therefore, to successfully obtain accurate identification of BRAF V600E positive ctDNA, assays must be capable of achieving single-nucleotide resolution.

There are several challenges associated with ctDNA analysis that preclude it from being widely implemented, particularly in resource-limited settings. The first challenge involves the isolation of ctDNA from plasma samples. Traditional extraction methods rely on silica-based sorbents that can require complex vacuum apparatuses, organic solvents (e.g., isopropanol and ethanol), and significant user intervention. Furthermore, commonly used detection methods such as digital PCR and qPCR, while highly sensitive, require

Received: November 25, 2019 Accepted: January 17, 2020 Published: January 17, 2020



sophisticated thermal cycling equipment and complex fluorescence detection modules.

Solid-phase microextraction (SPME) was developed as an alternative to traditional solid-phase extraction (SPE).¹² It relies on a thin sorbent film immobilized on a support that preconcentrates desired analytes from a sample. Advantages of SPME over traditional SPE include ease of automation, low cost, and short analysis times.¹³ Recently, SPME sorbent coatings comprised of polymeric ionic liquids (PILs) have been developed and applied for the analysis of ultraviolet filters,¹⁴ organophosphorous pesticides,¹⁵ and free fatty acids¹⁶ from a variety of matrices. Our group has utilized PIL-SPME for the rapid isolation and detection of nucleic acids from aqueous cell lysates and artificial sputum samples.^{17–19} PIL-SPME holds promise as a rapid, user-friendly technique for the isolation of ctDNA from plasma for subsequent molecular analysis.

Loop-mediated isothermal amplification (LAMP) is a powerful isothermal amplification technique capable of amplifying nucleic acid sequences with equal or better sensitivity than traditional PCR-based methods and shorter analysis times (<1 h).²⁰ Due to its rapid and isothermal nature, LAMP is a promising substitute for PCR, particularly in resource-limited settings. While possessing several advantages over PCR-based methods, LAMP does not have a universal sequence-specific detection method analogous to the TaqMan probe in qPCR. As a result, sequence-specific methodologies are highly desired, particularly for ctDNA analysis where single-nucleotide resolution is required.

Sequence-specific detection following LAMP amplification is a challenge that has been addressed through a variety of strategies including the incorporation of additional enzymes, use of competitive primers, strand displacement probes, and molecular beacons (MBs). MBs are dual-labeled oligonucleotide probes that can be designed to be highly specific to their target. Recently, our group demonstrated that MB-LAMP was capable of visually discriminating between single-nucleotide polymorphisms (SNPs). Due to its high specificity, MB-LAMP has the potential to be applied in ctDNA analysis.

In this study, we demonstrate for the first time the isolation of BRAF V600E ctDNA from human plasma samples using PIL-SPME and its subsequent LAMP detection using allelespecific MBs. The performance of PIL-SPME in plasma was systematically evaluated to identify the effects of protein, salt content, and anticoagulant used during plasma collection on the extraction of DNA. Furthermore, the utility of MB-LAMP for ctDNA analysis was expanded to demonstrate the positive identification of wild type and mutant sequences. The MB-LAMP reaction was also investigated with dual-labeled probes of various lengths to understand the relationship between the probe-structure and the observed fluorescence signal. Moreover, a plate reader assay capable of detecting 5% of the BRAF V600E mutation was developed and implemented, thereby eliminating the necessity of a qPCR instrument and increasing its potential as a point-of-care tool.

■ EXPERIMENTAL SECTION

Reagents and Instrumentation. All synthetic oligonucleotide primers and dual-labeled probes were purchased from Integrated DNA Technologies (Coralville, IA, U.S.A.). MBs and dual-labeled probes were prepared using HPLC purification while primers were ordered with standard

desalting. Tris(hydroxymethyl)aminomethane (Tris) and bovine serum albumin (BSA) were obtained from P212121 (Ypsilanti, MI, U.S.A.). Trisodium citrate, ethylenediaminetetraacetic acid dipotassium salt dihydrate, and dehydrated plasma were ordered from Sigma-Aldrich (St. Louis, MO, U.S.A.). Pooled human plasma apheresis derived was obtained from Innovative Research (Novi, MI, U.S.A.). Sodium chloride was obtained from Fisher Scientific (Hampton, NH, USA). Eppendorf Lobind centrifuge tubes (Hamburg, Germany) were used for all extractions. An Agilent Technologies Poroshell 120 column (50 mm \times 4.6 mm i.d. \times 2.7 μ m particle size) was used for BSA analysis. All fluorescence experiments were performed using a BioTek Synergy Hybrid H1 microplate reader. Deionized water (18.2 M Ω cm) used was obtained from a Millipore Milli-Q water purification system (Bedford, MA, U.S.A.). For BSA extraction experiments, an Agilent 1260 HPLC with a diode array detector coupled to an Agilent 6230B Accurate Mass Time of Flight (TOF) mass spectrometer with an electrospray source was

Template DNA Preparation. Three 3.9 kbp plasmids containing different insertions of 280, 210, and 210 bp were obtained from Eurofin Genomics (Louisville, KY, U.S.A.). The 280 bp fragment was employed in the extraction experiments. The two 210 bp fragments contained a portion of the BRAF gene. One fragment contained the BRAF V600E mutation while the other contained the wild type allele. All sequences, primers, and probes used in this study can be found in Table S1. PCR amplification of each inserted sequence was followed by agarose gel electrophoresis using a horizontal gel electrophoresis system H4 chamber from Bethesda Research Laboratories (Gaithersburg, MD) with a Neo/Sci (Rochester, NY) dual-output power supply. After electrophoresis, the amplicon bands were removed and purified by a QIAquick gel extraction kit (Qiagen, Hilden, Germany). The recovered DNA fragments were subsequently quantified by a NanoDrop 2000c spectrophotometer from Thermo Scientific (Waltham, MA) and stored at -20 °C.

qPCR Conditions. All qPCR experiments were carried out on a CFX96 Touch real-time PCR detection system from Bio-Rad Laboratories (Hercules, CA). The amplification protocol used for thermocycling was as follows: an initial denaturation step of 5 min at 95.0 °C followed by 40 cycles of 95.0 °C for 10 s and 58.0 °C for 30 s. All data points recorded were performed in triplicate unless otherwise specified. Each reaction contained the following reagents: 10 μ L (2X) SsoAdvanced Universal SYBR green supermix (Bio-Rad), 8.2 μ L of deionized water, 0.8 μ L of 10 μ M forward and reverse primers, and 1.0 μ L of template DNA.

PIL-SPME Extraction Procedure. Preparation of the PIL-SPME sorbents was performed following a previously reported method.²⁸ The chemical structure of the sorbent is shown in Figure S1. All extractions were carried out using the following procedure. A 1.0 mL volume of extraction solution containing 10 pg mL⁻¹ template DNA was pipetted into a 1.5 mL DNA LoBind tube. The cap of the tube was pierced using a needle to allow the PIL fiber to be immersed into the extraction solution upon closing. The centrifuge tube was then agitated with a Fisher-Brand digital vortex mixer (Fisher Scientific, Hampton, NH) for 2 min at 2500 rpm. Next, the fiber was removed from the extraction solution and washed in deionized water. After washing, the fiber was then transferred into 10 µL of 1 M NaCl (desorption solution) for 30 min. To alleviate qPCR inhibition

caused by the high salt concentration in the desorption solution, a 5-fold dilution was performed prior to qPCR analysis. Following desorption, the PIL fiber was placed in saturated (6.14 M) NaCl for 1 h prior to subsequent extractions.

Magnetic Bead Extractions. Extractions were performed using Dynabeads Myone Silane magnetic beads (Thermo-Fisher Scientific) as suggested by the manufacturer, with some modifications. Extraction solutions (1.0 mL) were prepared containing 10 pg mL⁻¹ DNA. A volume of 750 μ L of 6.0 M guanidine HCl was added to the extraction solution along with 30 μ L of beads (40 mg mL⁻¹ stock). The beads were subjected to vortex agitation for 2 min and were subsequently collected, washed with ethanol, and air-dried and the DNA was finally desorbed in 400 μ L of 2.0 mM Tris at pH 8.

LC-TOF-MS Conditions for BSA Analysis. LC-MS grade water (Fisher Scientific) supplemented with 0.1% formic acid (Sigma-Aldrich) was used as mobile phase A while acetonitrile with 0.1% formic acid was used as mobile phase B. An injection volume of 5.0 μ L was used. Gradient elution was performed using the following separation program: 5% B to 100% B from 0 to 10 min, held at 100% B from 10 to 15 min, decreased to 5% B from 15 to 20 min, and finally held at 5% B for 5 min.

An external calibration curve was prepared (Figure S2) by analyzing standard solutions of BSA and measuring the peak area obtained from the extracted ion chromatogram using the +50 charge state of the protein (1329.63 m/z)

LAMP Conditions. LAMP of the BRAF sequences was performed by heating at 60.5 °C for 1 h on a CFX96 Touch real-time PCR detection system. For real-time assays, fluorescence measurements were taken every 30 s. End-point fluorescence measurements were recorded using a BioTek Synergy Hybrid H1Microplate Reader (Winooski, VT). Each 10 μ L reaction mixture contained the following components: 1.4 mM of each dNTP (New England Biolabs, Ipswich, MA), 10× isothermal buffer (NEB), 6 mM MgSO₄ (NEB), 0.5 μ M wild type and mutant MBs, 1.6 μ M FIP and BIP primers, 0.2 μ M F3 and B3 primers, 0.4 μ M LoopB primer, 3200 U Bst 2.0 WarmStart DNA polymerase (NEB), and 1 μ L of template DNA solution.

■ RESULTS AND DISCUSSION

MB-LAMP Assay Design. During LAMP, single-stranded loop regions are generated between the F1 and F2 regions of the target DNA. These single-stranded loops are available for hybridization with the MB probe. For this assay, a primer set containing the V600E mutation between the F1 and F2 region of the target was designed using Primer Explorer V4.0 software. Initially, the molecular beacon (MB1) was created as described by Liu et al. As illustrated in Figure 1A, the loop primer was modified by adding additional bases to the 3' end to generate the MB stem. This design allows part of the stem to be fully hybridized to the target. However, as shown in Figure 1B, sufficient discrimination between the wild type and mutant sequences was not observed when this strategy was implemented. This was likely due to the location of the SNP in the last nucleotide of the 3' end of the loop primer.

Therefore, a different molecular beacon (MB2) was designed in order to obtain better discrimination. This was done by selecting a different loop primer and adding several nucleotides to generate the MB stem (Figure 1A). In this case, additional nucleotides were incorporated to both 5' and 3' ends of the loop primer, unlike MB1 which only had

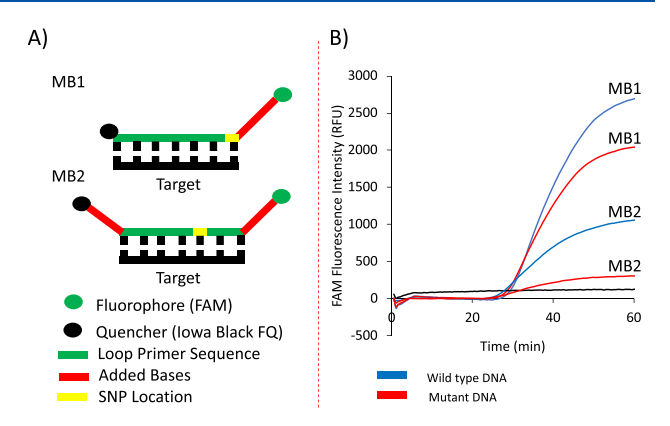


Figure 1. (A) Representative illustrations of the molecular beacons used to discriminate between wild type and mutant BRAF V600E sequences. (B) Real-time MB-LAMP amplification plots of wild type (blue) and mutant (red) BRAF in the presence of wild type (FAM labeled) MB1 or MB2.

nucleotides added to the 3' end. Figure 1B shows representative real-time amplification curves when this MB was used for the detection of the wild type and mutant sequences. Greater differentiation between the wild type and mutant sequence was observed when MB2 was used compared to MB1. Annealing profiles between MB2 and its complementary sequence are shown in Figure S3 and confirm the ability of MB2 to discriminate between wild type and mutant sequences.

The reaction temperature is an important parameter to optimize in order to obtain sufficient discrimination between wild type and mutant sequences. Reactions were performed using several temperatures ranging from 60 to 62.8 °C. Representative amplification plots in Figure S4 show that 60.5 °C affords the highest fluorescence for the wild type sequence while maintaining discrimination from the mutant sequence. Subsequently, the concentration of the MB in the reaction was optimized. It was found that 0.5 μ M MB yielded the highest fluorescence after amplification of the wild type sequence (Figure S5A–C).

Previous studies have suggested that 0.8 M betaine was required in the MB-LAMP assay, potentially limiting its usefulness due the destabilizing nature of the zwitterionic molecule. Betaine is often used as a qPCR and LAMP additive for the amplification of GC-rich regions as it decreases the stability of GC base pairs to be similar to AT base pairs. In order to determine whether betaine was an essential component of the MB-LAMP reaction mixture, reactions were performed without it. As shown in Figure S6, the reaction progressed even in the absence of betaine. Moreover, the removal enabled a higher maximum fluorescence signal in the presence of the target. Sufficient discrimination was also obtained when betaine was removed, indicating that SNP detection could still be achieved. These results strongly suggest that betaine is not a requisite component of MB-LAMP assays.

In order to detect both wild type and mutant sequences independently, a second MB targeting the mutant allele was incorporated into the assay. This MB was structurally similar to MB2 with the exception of using HEX (mutant) as the reporter dye instead of FAM (wild type). A representative illustration of the MBs used in the assay is shown in Figure 2A. Real-time reactions were performed using the multiplexed assay and representative homozygous mutant, homozygous

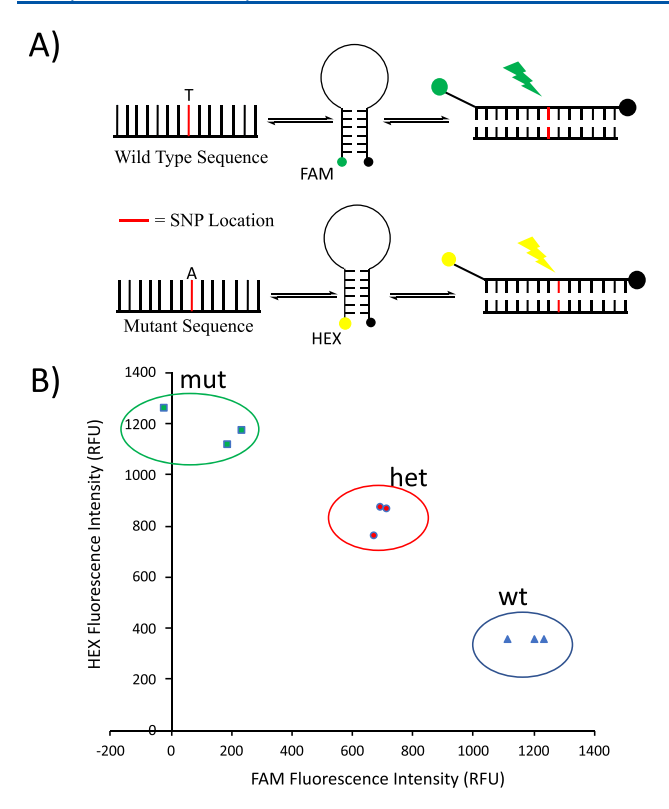


Figure 2. (A) General schematic of the molecular beacons used in this study to identify wild type (FAM) and mutant (HEX) BRAF sequences. (B) Allelic discrimination plot derived from end point fluorescence measurements obtained from the qPCR instrument.

wild type, and heterozygous samples. Figure 2B demonstrates the capability of the assay for allelic discrimination. Discrete populations of each genotype are clearly observed when the end point fluorescence of each channel obtained from qPCR (FAM and HEX channels) is plotted for each reaction performed.

End Point Detection Using a Plate Reader. One significant advantage of LAMP over traditional qPCR-based techniques is cost effectiveness. LAMP can be performed without sophisticated thermal-cycling equipment or expensive fluorescence modules that are often required for qPCR. Due to the real-time monitoring inherent to qPCR, it is necessary to obtain fluorescence measurements after every amplification cycle performed. In order to design the MB-LAMP assay to be more amenable for point-of-care applications, a plate reader was proposed as an alternative to the qPCR instrument for end-point detection and discrimination, thereby reducing assay costs.

To determine the feasibility of using a plate reader for end point detection, triplicate reactions containing either the wild type or mutant sequence and no template controls (NTCs) were performed. Following amplification at 60.5 °C, a plate reader was used to obtain end point fluorescent readings of the HEX (excitation λ , 530 nm; emission λ , 560 nm) and FAM (excitation λ , 485 nm; emission λ , 528 nm) probes for each reaction performed. Figure S7A illustrates the fluorescence values obtained for the HEX and FAM channels for each reaction. In order to more clearly visualize discrimination of the two sequences, Figure S7B plots the fluorescence values of HEX and FAM channels from each reaction performed. This graph shows a clear separation between the mutant, wild type,

and NTC reactions indicating the viability of the plate reader as an alternative detection method.

Mutant ctDNA sequences comprise a small percentage of the total amount of cell-free DNA present in plasma. Therefore, it is necessary to assess whether the plate reader could detect the mutant sequence in the presence of excess wild type sequence. MB-LAMP reactions containing 2.34 \times 10⁵ copies μL^{-1} of the BRAF fragment (wild type + mutant) were carried out with either 1%, 5%, or 10% of the mutant sequence. Fluorescence measurements obtained from the plate reader assay are shown in Figure 3. These results indicate that

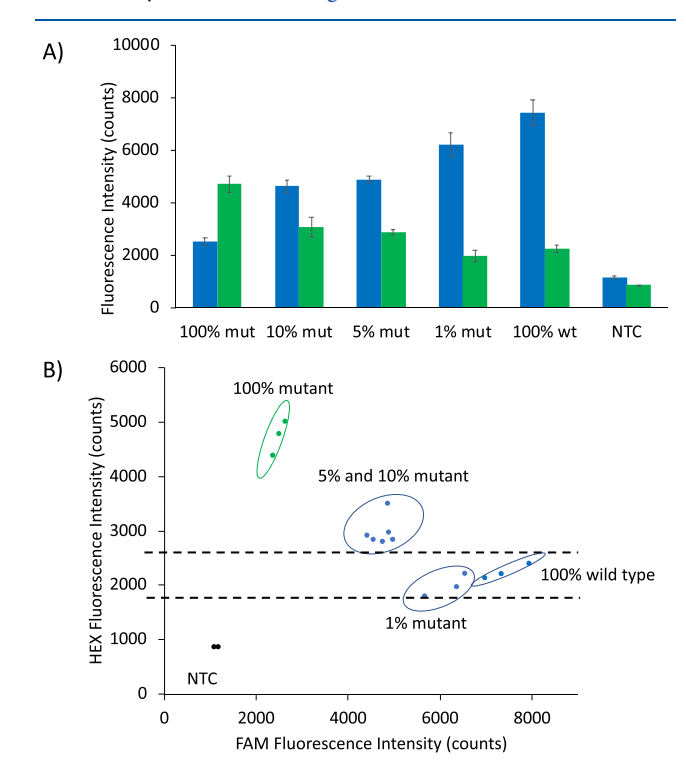


Figure 3. (A) Fluorescence values obtained using the plate reader from reactions containing 2.34×10^5 copies μL^{-1} of the BRAF fragment with different percentages of the mutant sequence. (B) Fluorescence plot illustrating the mutant positive reactions. The dotted line represents a 95% confidence interval created using the average HEX value for the 100% wild type reactions. Blue columns represent FAM fluorescence while green columns represent HEX.

the MB-LAMP can detect down to 5% of the mutant BRAF sequence when the plate reader is used. In comparison, traditional Sanger sequencing can typically detect 15–20% of the mutant sequence, pyrosequencing can detect down to 2%, and modified PCR-based methods can detect down to 0.1%. Probe-based LAMP methods such as one-step strand displacement (OSD)-LAMP have reported similar results to the developed assay (5%).

Investigation of Probe Structure and Its Effect on the Resulting Fluorescence. Careful design of the MB is essential for obtaining single-nucleotide specificity and sufficient fluorescence for identification of positive reactions. As mentioned previously, MB1 was designed as described by Liu et al. and did not afford significant discrimination between the wild type and mutant sequences. However, it was observed that the fluorescence values obtained with MB1 and the wild-type sequence were higher than MB2. The length of the two MBs are similar, with MB1 and MB2 containing 24 and 23

nucleotides, respectively. During stem design, seven additional nucleotides were added onto the 3' end to create the stem, allowing the 5' end to fully hybridize with the target. MB2 was designed by adding nine additional nucleotides to the loop primer, four nucleotides to the 5' end, and five nucleotides to the 3' end.

Due to the formation of single-stranded DNA loops during LAMP amplification, it is possible that hybridization of the MB to the loop structure could allow the fluorophore-quencher pair to interact in space, leading to quenching by FRET. To test this, the length of MB2 (32 nt) was modified by reducing the length to 30, 28, and 23 nt. LAMP reactions were performed with each sequence, as previously optimized, and FAM fluorescence recorded using the plate reader. As shown in Figure 4, a noticeable increase in fluorescence was observed

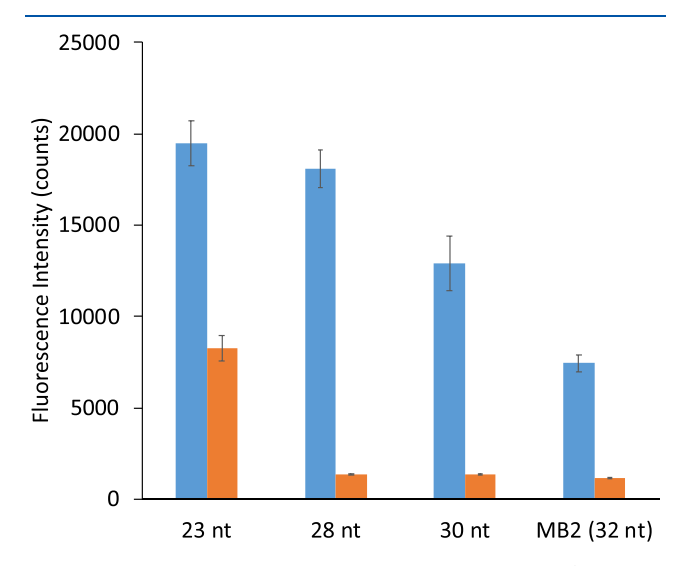


Figure 4. Fluorescence measurements of the FAM channel (excitation λ , 485 nm; emission λ , 528 nm) following LAMP amplification with different length of dual-labeled probes. The blue bars represent the positive reactions while the orange bars the NTCs. Triplicate reactions were performed for each probe.

as the length of the probe decreased. These results suggest that quenching of MB2 could be responsible for the decreased fluorescence when compared to MB1. When designing MBs for LAMP applications, decreasing the number of added nucleotides to the loop primer may lead to higher fluorescence values. Studies are ongoing in our laboratory to understand if these observations can be generalized to all MB-LAMP assays.

SPME Preconcentration from Plasma. PIL-SPME has previously been applied in a variety of complex samples (cell lysate and artificial sputum) for the extraction of nucleic acids. 17,19 To determine the feasibility of PIL-SPME for DNA isolation from plasma, extractions were performed from plasma that was collected and stored using the anticoagulant trisodium citrate (4%). All extractions were performed using a 280 bp sequence at clinically relevant ctDNA concentrations (10 pg $mL^{-1} = 54.94$ fM). As observed in Figure 5A, there was an approximate 6 quantification cycle (Cq) increase when the extraction was performed from the plasma (31.49 \pm 0.58) compared to 2.0 mM tris buffer pH 8.0 (25.21 \pm 0.28). For reference, a Cq value increase of 1 indicates a 2-fold decrease in the amount of DNA present in the reaction under optimal reaction conditions.³⁶ This increase in Cq value indicates that some component of the plasma significantly affected the

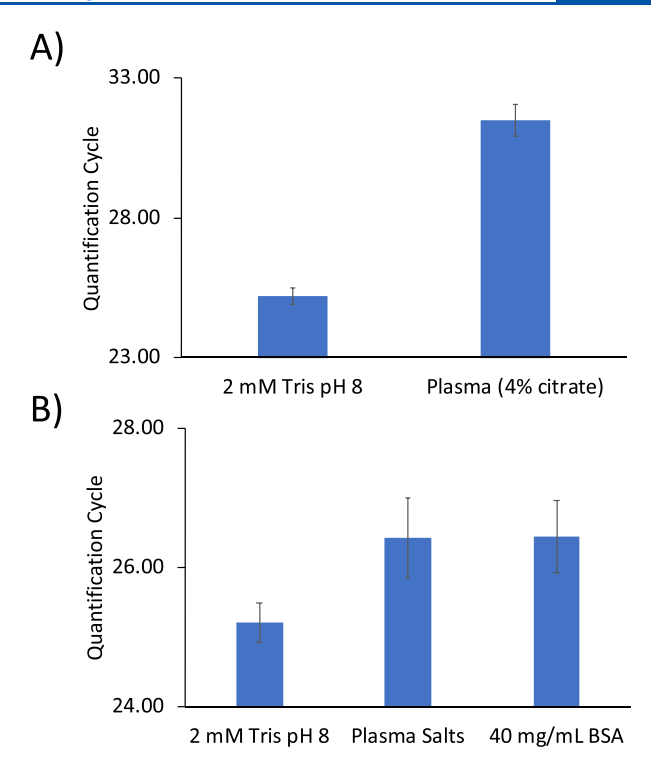


Figure 5. qPCR results following PIL-SPME of a model 280 bp DNA from different matrices. (A) Comparison of extractions from Tris buffer and plasma containing 4.0% trisodium citrate. (B) Evaluation of the salts from plasma as well as protein on the extraction of DNA.

extraction or inhibited the qPCR reaction. It is important to emphasize that direct addition of the plasma to qPCR yielded no observable amplification. Therefore, these results demonstrate PIL-SPME as a useful technique for the isolation and preconcentration of sufficiently pure nucleic acid for qPCR analysis.

To determine whether the plasma was causing inhibition of qPCR, the extraction procedure was performed without any DNA in the plasma, allowing the SPME sorbent coating to extract potential inhibitors. A 10 fg mass of target DNA was subsequently added to the desorption solution after 30 min, diluted 5-fold, and analyzed by qPCR. This was compared to an identical procedure using Tris buffer instead of the plasma and spiking the same amount of DNA into the desorption solution. As shown in Figure S8, amplification of the two solutions was identical, indicating that no inhibitory components were coextracted by the PIL fiber from the plasma. These data strongly suggest that the higher Cq values observed are due to a component of the plasma affecting the extraction process, not qPCR inhibition by plasma components

Various salts responsible for maintaining osmotic balance in the plasma are potential culprits that are known to influence the DNA extraction process. Since PIL-based sorbent coatings predominantly extract DNA through an ion exchange mechanism, it is possible that higher ionic strength extraction solutions can affect interactions between the sorbent and DNA. To determine the effect of these salts on the extraction, a solution was prepared to mimic the salts present in plasma. Extractions were performed from this salt solution, resulting in Cq values (26.43 ± 0.52) higher than those from Tris (25.21 ± 0.28) , as shown in Figure 5B. These results suggest that the salts present in plasma can cause a moderate decrease in the

extraction. However, the observed Cq value difference of 1.22 is significantly lower than the 6.28 cycle difference between Tris and plasma extractions.

Protein represents another major component of plasma that has the potential to negatively affect PIL-SPME. Figure 5B demonstrates the results obtained following extractions from a 40 mg mL $^{-1}$ BSA solution mimicking the concentration of serum albumin in plasma. The Cq values from these extractions (26.45 \pm 0.57) were very similar to those obtained from extractions performed from the salt solution. These results suggest possible coextraction of protein by the PIL, which could cause a competitive effect with DNA for ion-exchange sites on the fiber coating.

There are various species of anticoagulants that can be employed during plasma collection and storage. The plasma used in previous experiments contained 4.0% trisodium citrate, resulting in a concentration of 155 mM. It is possible that the high concentration of anionic species such as citrate could reduce the strength of electrostatic interactions between the PIL sorbent coating and DNA. To investigate this, extractions were performed from a 4.0% trisodium citrate solution containing the different plasma salts. The Cq values obtained (31.81 ± 0.46) were comparable to those obtained from extractions of human plasma (31.49 ± 0.58) collected with 4.0% trisodium citrate.

It was hypothesized that using a different anticoagulant such as K2EDTA or Na2EDTA could enable lower Cq values to be achieved. However, extractions performed from plasma collected using K2EDTA and Na2EDTA yielded nearly identical results as the citrate-treated plasma (data not shown). To determine whether the presence of the EDTA was responsible for increased Cq values, extractions were performed using 4.0 mM K2EDTA in a solution containing the plasma salts. The Cq values obtained (26.45 \pm 0.45) from these extractions were not significantly different than those performed in the salt solution (26.43 \pm 0.52). These data indicate that another component of the plasma is responsible for affecting the extraction behavior of the PIL sorbent.

Since the PIL sorbent was affected by the components in the plasma, it is possible that commercially available DNA extraction materials also exhibit negative effects when used in plasma. The extraction performance of PIL-SPME was compared with that of magnetic beads for DNA extraction from Tris buffer and K2EDTA plasma. Figure S9 compares the extraction results of PIL-SPME and the magnetic beads. Interestingly, the Cq values are nearly identical for both methods in the two different sample matrices. These results show that reduced performance in plasma also occurs with silica-based extraction techniques.

Effects of Protein on PIL-SPME DNA Extractions. Interactions between the PIL-SPME sorbent coating evaluated in this study and protein have not been previously investigated. Due to the lower DNA extraction achieved from the BSA solution, it was hypothesized that protein could interact with the PIL coating. In order to evaluate the interaction of the PIL sorbent with BSA, extractions were performed from a 40 mg mL⁻¹ BSA solution and the desorption solution subsequently analyzed by LC-TOF-MS. Using an external calibration curve for quantification (Figure S2), it was determined that the sorbent extracted 4.11 \pm 0.61 μ g of BSA.

The effect of BSA on the qPCR efficiency was subsequently studied. As established by the MIQE guidelines, ³⁶ acceptable

qPCR efficiencies range from 90 to 110% and are obtained using eq 1.

$$efficiency = [10^{-1/slope} - 1] \times 100$$
 (1)

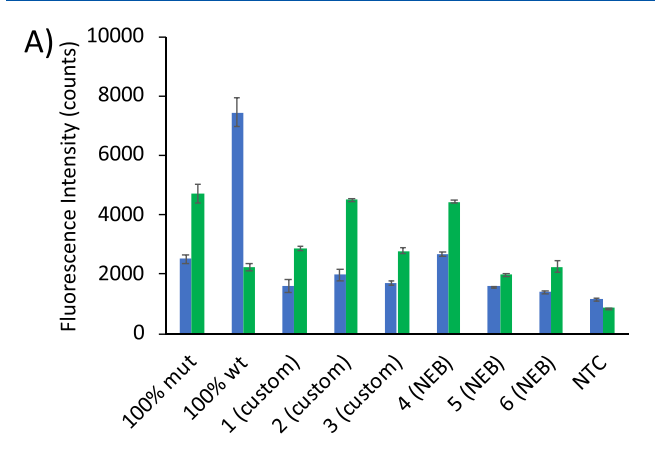
An efficiency of 100% indicates the doubling of DNA during every qPCR cycle. DNA extractions were performed at four different DNA concentration levels in solutions containing 40 and 4.0 mg mL $^{-1}$ BSA. Figure S10 shows the efficiency of the calibration curves to be 90.64% and 99.91% from the 40 and 4 mg mL $^{-1}$ BSA solutions, respectively. These results indicate that while high BSA concentrations cause a decrease in the qPCR efficiency, the obtained values remain within acceptable limits.

Extractions of BRAF V600E from Plasma for MB-LAMP Detection. The applicability of PIL-SPME for the isolation of clinically relevant ctDNA sequences from plasma for subsequent MB-LAMP analysis was explored. Briefly, 1.0 mL of K2EDTA plasma was spiked with 10 pg of the BRAFV600E fragment corresponding to a clinically relevant concentration (73.26 fM) of the mutant sequence. PIL-SPME was performed and the desorption solution analyzed using MB-LAMP with the plate reader, as previously described. To prevent any dilution of the desorption solution, a previously optimized MB-LAMP buffer was used. 19

Figure 6A shows the fluorescence results using the plate reader following PIL-SPME from the spiked plasma sample. Following triplicate extractions, the custom-buffer enabled the detection of all extractions performed. A comparison was also performed using the isothermal buffer provided by New England Biolabs. Due to the high salt concentration of the desorption solution, a 10-fold dilution prior to analysis must be performed. Two of the reactions were unable to be positively identified as BRAF V600E due to the required dilution. These results can be more clearly seen in Figure 6B where the HEX fluorescence of these reactions does not rise above the set threshold. This indicates the custom-buffer is a necessary component for the successful coupling of PIL-SPME with MB-LAMP.

■ CONCLUSIONS

In summary, a MB-LAMP assay was designed and implemented to enable detection of the clinically relevant BRAF V600E mutation. To simplify the application of the assay in resource-limited settings for point-of-care applications, a plate reader was used for detection. During assay development, dual-labeled probes (fluorophore-quencher) of different lengths were employed to investigate the relationship between the probe structure and the observed fluorescence. These experiments will serve as a guide in future MB design for LAMP applications. Furthermore, PIL-SPME was utilized as a simple, centrifuge-free sample preparation technique for the isolation of DNA from human plasma samples in clinically relevant concentrations. The effects of various plasma components on the extraction was also systematically evaluated. Future work will focus on lowering the cost of the assay by implementing a water bath for amplification and smartphone-based detection. Furthermore, to make the current method more user-friendly, the number of steps can be reduced by using lyophilized reagents. This study demonstrates the potential of MB-LAMP for the detection of ctDNA mutations and further expands the use of PIL-SPME for DNA extraction from complex biological samples.



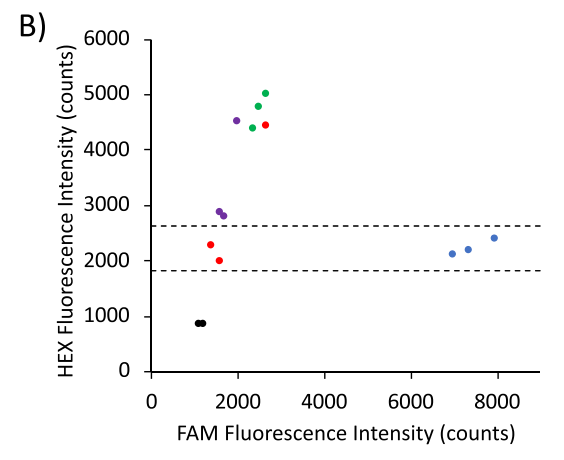


Figure 6. (A) Fluorescence results following PIL-SPME with MB-LAMP detection performed in the custom-buffer or NEB's isothermal buffer. Blue columns represent FAM fluorescence while green columns represent HEX. (B) Plot generated using the values obtained from the fluorescence readings following MB-LAMP for each extraction performed. Fluorescence values from 100% wild type reactions (blue) and 100% mutant reactions (green) were used as a control. Reactions performed in the custom buffer are visualized in purple while the isothermal buffer reactions are in red. The dotted line represents a 95% confidence interval created using the average HEX value for the 100% wild type reactions.

ASSOCIATED CONTENT

Supporting Information

The Supporting Information is available free of charge at https://pubs.acs.org/doi/10.1021/acs.analchem.9b05323.

DNA sequences and oligonucleotide probes used. PIL chemical composition, BSA LC-MS calibration curve, MB-annealing profiles, real-time LAMP plots optimizing temperature, MB concentration, and betaine; end-point results using a plate reader; comparison of PIL-SPME and magnetic beads; and calibration curves from plasma (PDF)

AUTHOR INFORMATION

Corresponding Author

Jared L. Anderson — Department of Chemistry, Iowa State University, Ames, Iowa 50011, United States; o orcid.org/0000-0001-6915-8752; Email: andersoj@iastate.edu

Authors

Marcelino Varona — Department of Chemistry, Iowa State University, Ames, Iowa 50011, United States **Derek R. Eitzmann** – Department of Chemistry, Iowa State University, Ames, Iowa 50011, United States

Darshna Pagariya — Department of Chemistry, Iowa State University, Ames, Iowa 50011, United States

Robbyn K. Anand — Department of Chemistry, Iowa State University, Ames, Iowa 50011, United States; orcid.org/ 0000-0003-2801-8280

Complete contact information is available at: https://pubs.acs.org/10.1021/acs.analchem.9b05323

Notes

The authors declare no competing financial interest.

ACKNOWLEDGMENTS

Research reported in this manuscript was supported by the Chemical Measurement and Imaging Program at the National Science Foundation (Grant No. CHE-1709372) and the National Institutes of Biomedical Imaging and Bioengineering of the National Institutes of Health under award number R21EB028583.

REFERENCES

- (1) Hiom, S. C. Br. J. Cancer 2015, 112, S1-S5.
- (2) Heitzer, E.; Ulz, P.; Geigl, J. B. Clin. Chem. 2015, 61, 112-123.
- (3) Gorgannezhad, L.; Umer, M.; Islam, M. N.; Nguyen, N. T.; Shiddiky, M. J. A. Lab Chip 2018, 18, 1174–1196.
- (4) Hamburg, M. A.; Collins, F. S. N. Engl. J. Med. 2010, 363, 301–304.
- (5) Flaherty, K. T.; Yasothan, U.; Kirkpatrick, P. Nat. Rev. Drug Discovery 2011, 10, 811-812.
- (6) Flaherty, K. T.; Puzanov, I.; Kim, K. B.; Ribas, A.; McArthur, G. A.; Sosman, J. A.; O'Dwyer, P. J.; Lee, R. J.; Grippo, J. F.; Nolop, K.; Chapman, P. B. N. Engl. J. Med. 2010, 363, 809–819.
- (7) Davies, H.; Bignell, G. R.; Cox, C.; Stephens, P.; Edkins, S.; Clegg, S.; Teague, J.; Woffendin, H.; Garnett, M. J.; Bottomley, W.; Davis, N.; Dicks, E.; Ewing, R.; Floyd, Y.; Gray, K.; Hall, S.; Hawes, R.; Hughes, J.; Kosmidou, V.; Menzies, A.; Mould, C.; Parker, A.; Stevens, C.; Watt, S.; Hooper, S.; Wilson, R.; Jayatilake, H.; Gusterson, B. A.; Cooper, C.; Shipley, J.; Hargrave, D.; Pritchard-Jones, K.; Maitland, N.; ChenevixTrench, G.; Riggins, G. J.; Bigner, D. D.; Palmieri, G.; Cossu, A.; Flanagan, A.; Nicholson, A.; Ho, J. W. C.; Leung, S. Y.; Yuen, S. T.; Weber, B. L.; Seigler, H. F.; Darrow, T. L.; Paterson, H.; Marais, R.; Marshall, C. J.; Wooster, R.; Stratton, M. R.; Futreal, P. A. Nature 2002, 417, 949—954.
- (8) Paik, P. K.; Arcila, M. E.; Fara, M.; Sima, C. S.; Miller, V. A.; Kris, M. G.; Ladanyi, M.; Riely, G. J. *J. Clin. Oncol.* **2011**, 29, 2046–2051.
- (9) Lee, H.; Na, W.; Park, C.; Park, K. H.; Shin, S. Sci. Rep. 2018, 8, 5467.
- (10) Stemmer, C.; Beau-Faller, M.; Pencreac'h, E.; Guerin, E.; Schneider, A.; Jaqmin, D.; Quoix, E.; Gaub, M. P.; Oudet, P. Clin. Chem. **2003**, 49, 1953–1955.
- (11) Pratt, E. D.; Cowan, R. W.; Manning, S. L.; Qiao, E.; Cameron, H.; Schradle, K.; Simeone, D. M.; Zhen, D. B. *Anal. Chem.* **2019**, *91*, 7516–7523.
- (12) Arthur, C. L.; Pawliszyn, J. Anal. Chem. 1990, 62, 2145-2148.
- (13) Kasperkiewicz, A.; Gómez-Ríos, G. A.; Hein, D.; Pawliszyn, J. Anal. Chem. 2019, 28, 59.
- (14) An, J.; Anderson, J. L. Talanta 2018, 182, 74-82.
- (15) Gionfriddo, E.; Souza-Silva, É. A.; Ho, T. D.; Anderson, J. L.; Pawliszyn, J. *Talanta* **2018**, *188*, 522–530.
- (16) Pacheco-Fernández, I.; Trujillo-Rodríguez, M. J.; Kuroda, K.; Holen, A. L.; Jensen, M. B.; Anderson, J. L. *Talanta* **2019**, 200, 415–423.
- (17) Nacham, O.; Clark, K. D.; Anderson, J. L. Anal. Chem. 2016, 88, 7813-7820.

- (18) Nacham, O.; Clark, K. D.; Varona, M.; Anderson, J. L. Anal. Chem. 2017, 89, 10661–10666.
- (19) Varona, M.; Ding, X.; Clark, K. D.; Anderson, J. L. Anal. Chem. **2018**, 90, 6922–6928.
- (20) Notomi, T.; Okayama, H.; Masubuchi, H.; Yonekawa, T.; Watanabe, K.; Amino, N.; Hase, T. *Nucleic Acids Res.* **2000**, 28, E63.
- (21) Fu, Y.; Duan, X.; Huang, J.; Huang, L.; Zhang, L.; Cheng, W.; Ding, S.; Min, X. Sci. Rep. **2019**, 9, 42542 DOI: 10.1038/s41598-019-42542-x.
- (22) Malpartida-Cardenas, K.; Rodriguez-Manzano, J.; Yu, L. S.; Delves, M. J.; Nguon, C.; Chotivanich, K.; Baum, J.; Georgiou, P. *Anal. Chem.* **2018**, *90*, 11972–11980.
- (23) Cai, S.; Jung, C.; Bhadra, S.; Ellington, A. D. Anal. Chem. 2018, 90, 8290–8294.
- (24) Jiang, Y. S.; Bhadra, S.; Li, B.; Wu, Y. R.; Milligan, J. N.; Ellington, A. D. Anal. Chem. 2015, 87, 3314–3320.
- (25) Liu, W.; Huang, S.; Liu, N.; Dong, D.; Yang, Z.; Tang, Y.; Ma, W.; He, X.; Ao, D.; Xu, Y.; Zou, D.; Huang, L. Sci. Rep. **2017**, 7, 40125.
- (26) Mhlanga, M. M.; Malmberg, L. Methods 2001, 25, 463-471.
- (27) Varona, M.; Anderson, J. L. Anal. Chem. 2019, 91, 6991-6995.
- (28) Ho, T. D.; Toledo, B. R.; Hantao, L. W.; Anderson, J. L. Anal. Chim. Acta 2014, 843, 18–26.
- (29) Nanayakkara, I. A.; White, I. M. Analyst 2019, 144, 3878-3885.
- (30) Becherer, L.; Bakheit, M.; Frischmann, S.; Stinco, S.; Borst, N.; Zengerle, R.; Von Stetten, F. *Anal. Chem.* **2018**, *90*, 4741–4748.
- (31) Rees, W. A.; Korte, J.; Von Hippel, P. H.; Yager, T. D. *Biochemistry* **1993**, 32, 137–144.
- (32) Kelley, S. O. ACS Sensors 2017, 2, 193-197.
- (33) Lee, S. T.; Kim, S. W.; Ki, C. S.; Jang, J. H.; Shin, J. H.; Oh, Y. L.; Kim, J. W.; Chung, J. H. *J. Clin. Endocrinol. Metab.* **2012**, *97*, 2299–2306.
- (34) Huang, T.; Zhuge, J.; Zhang, W. W. Biomark. Res. 2013, 1, 3.
- (35) Johansson, M. K.; Fidder, H.; Dick, D.; Cook, R. M. J. Am. Chem. Soc. 2002, 124, 6950–6956.
- (36) Huggett, J. F.; Foy, C. A.; Benes, V.; Emslie, K.; Garson, J. A.; Haynes, R.; Hellemans, J.; Kubista, M.; Mueller, R. D.; Nolan, T.; Pfaffl, M. W.; Shipley, G. L.; Vandesompele, J.; Wittwer, C. T.; Bustin, S. A. Clin. Chem. 2013, 59, 892–902.
- (37) Tan, S. C.; Yiap, B. C. J. Biomed. Biotechnol. 2009, 2009, 1-10.
- (38) Przondziono, J.; Walke, W.; Hadasik, E.; Młynarski, R. Adv. Mater. Sci. Eng. 2013, 2013, 1–6.